

Multiphoton excitation of high singlet np Rydberg states of molecular hydrogen: Spectroscopy and dynamics

Wallace L. Glab and Jan P. Hessler

Chemistry Division, Argonne National Laboratory, Argonne, Illinois 60439

(Received 23 October 1986)

We have used two-step, two-color excitation to populate high np singlet Rydberg states of molecular hydrogen under electric-field-free conditions. Sub-Doppler resolution is obtained by exciting the $X^1\Sigma_g^+ \rightarrow E^1\Sigma_g^+$ two-photon transition with copropagating photons, then further exciting the molecules to high Rydberg states with a narrow-band laser. We have observed transitions to states up to $n \sim 90$ for the Rydberg series which converge to the two lowest ionization limits. From an analysis of the energies of the observed transitions we have obtained new results for the first two ionization potentials of molecular hydrogen, with the highest accuracy reported to date. The new values are $124\,417.61 \pm 0.07 \text{ cm}^{-1}$ for parahydrogen and $124\,475.94 \pm 0.07 \text{ cm}^{-1}$ for orthohydrogen. Some of the Rydberg states predissociate strongly, apparently due to the influence of perturbing states of low principle quantum number. This is the first observation of such predissociation in Rydberg states of high principle quantum number.

Although the spectroscopic and dynamic properties of high Rydberg states of atomic systems are mostly well understood, the properties of high Rydberg states of even the simplest molecule, molecular hydrogen, present many unanswered questions. The principle difficulty in carrying our knowledge about atomic Rydberg states over to molecular systems lies in the fact that a molecular ion core has vibrational and rotational degrees of freedom. Each of the closely spaced rovibrational levels of the core is the limit of a Rydberg series; therefore, the molecule has a large number of interacting Rydberg series which greatly complicate the analysis of spectra. The additional degrees of freedom of the core also lead to dynamical processes which are not possible in atomic systems, such as dissociation and vibrational autoionization.

Analysis of the energies of the states in Rydberg series has long been used in the determination of the ionization potentials of atomic and molecular species. Accurate experimental results for the values of the ionization potentials of the hydrogen molecule are important in that they determine experimental values for the molecular constants of the molecular ion. The dissociation energy of the molecular ground state can also be determined from ionization potentials, when combined with accurate values for the energy of the ground state of the molecular ion. The first studies of the Rydberg states of molecular hydrogen made use of single-photon absorption from the ground state to study the singlet np Rydberg series.¹⁻⁴ These studies have yielded such information as quantum defects and series limits for this series and examined autoionizing states; however, the relatively low spectral resolution of these studies limited the accuracy of the results. Absorption studies such as these have yielded only very limited information about the dynamics of the highly excited molecules, since they rely on the resolution of line shapes. Experiments of this kind are insensitive to processes with rates $< 10^{11} \text{ s}^{-1}$; moreover, they do not directly discrim-

inate between different decay channels such as autoionization and predissociation. Predissociation has been observed directly through detection of fluorescence from excited atomic products, but only for states of relatively low principle quantum number ($n < 10$).⁵

Recently, laser excitation has been used in a number of studies of high Rydberg states of molecular hydrogen. The nd and nf triplet series have been examined by several groups,⁶⁻⁸ one of which has very recently reported a new value for the first ionization potential of H_2 .⁸ Autoionizing states of the singlet np series have been studied at improved resolution using multiphoton excitation,⁹ and the singlet ns and nd series have been excited to a principle quantum number of $n \sim 75$.¹⁰ At present the spectral resolution of these experiments has generally been limited to a few tenths of a wave number or greater, either by the Doppler width of the transitions or the spectral width of the laser source, and although one of the experiments¹⁰ was sensitive to dissociation it did not discriminate between dissociation and ionization as decay channels of the excited population.

In this paper we describe the use of two-step, two-color excitation through the two-photon-resonant $E^1\Sigma_g^+$ ($v=0, J=0,1$) state to populate high-lying singlet np Rydberg states of molecular hydrogen which converge to the $v=0$ level of the ion core. Since these states cannot autoionize, the transitions are very sharp and their energies can be measured very accurately. We used a narrow-bandwidth light source to drive the $X \rightarrow E$ transition through the absorption of two copropagating photons, resulting in the selective excitation of molecules with a narrow range of velocity components. A second narrow-bandwidth laser is then tuned over the Rydberg series, producing further excitation to high Rydberg states with linewidths much less than the Doppler width. We have used this technique to measure the energies of the high singlet np states of both para- and orthohydrogen with

high accuracy. By combining an analysis of these results with accurate measurements of the $X \rightarrow E$ transition energies we have derived precise new values for the $v=0$, $N=0,1$ series limits and the quantum defects for the series. In addition, we have observed directly, for the first time, significant predissociation of the high Rydberg states. To accomplish this, Balmer- α light from a third tunable laser was used to ionize the dissociation products. A field-free drift tube provided mass selective detection, thereby providing information on both the ionization and dissociation channels.

I. EXPERIMENT

Resonant multiphoton excitation of molecules has recently emerged as a very important method of gaining information on the spectroscopic and dynamical properties of molecules. This technique provides a means of exciting states which are inaccessible from the ground state via single-photon absorption due to their high excitation energy, poor Frank-Condon factors, or symmetry. Hydrogen has been studied recently using one- and three-photon excitation of the B or C state followed by further excitation,¹⁰⁻¹² and also by two- and four-photon excitation of the E state.^{9,13,14} In the study described here, we have used two-step, two-color excitation with the two-photon transition to the $v=0$, $J=0,1$ levels of the E state as the first step.

Figure 1 shows the relevant potential curves of the hy-

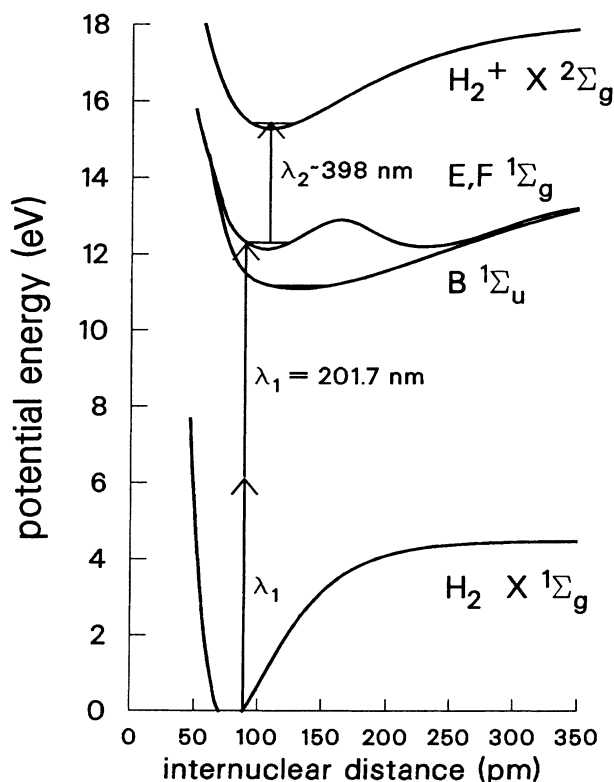


FIG. 1. Relevant potential curves of the hydrogen molecule, showing the excitation scheme used in the experiment.

drogen molecule. Excitation from the $X^1\Sigma_g^+$ ($v=0, J=0$) level to the $E^1\Sigma_g^+$ ($v=0, J=0$) level occurs with the simultaneous absorption of two photons with a wavelength of 201.7 nm. Once in the E state the molecule can decay by fluorescence to the B state or through collisional transfer to the C state which then fluoresces. The lifetime of this level of the E state has recently been determined to be 200 ns.¹⁵ After a delay of several nanoseconds, light from a second laser tunable near 398 nm promotes a fraction of the excited molecules to high np Rydberg states. The molecules excited to Rydberg states may then decay through a number of possible channels. The molecules may decay by fluorescence to a lower state; however, since the radiative lifetimes of high Rydberg states¹⁶ are much longer than the observation times in our experiment (~ 100 ns), we will neglect this decay channel in future discussions. Autoionization may occur if the energy of the state is above the lowest ionization limit of the molecule; also, the molecule in a Rydberg state may be ionized by collisions or by electric fields. These processes all lead to production of the molecular ion, which is detected in the experiment. In addition, it is energetically possible for the high Rydberg molecule to undergo predissociation, leading to the production of a ground-state hydrogen atom and an atom in an $n=2$ state. There is insufficient energy in the region of the ionization potential for dissociation into a ground-state atom plus an atom in an $n=3$ state. Predissociation is expected to be weak for Rydberg states of very high principle quantum number due to their very small overlap with the ionic core, and has only been observed for states with $n < 10$. Detailed theoretical calculations for relatively low principle quantum numbers have shown that predissociation rates drop off rapidly with increasing principle quantum number.¹⁷ Predissociation of this type may be detected by ionizing the excited hydrogen atoms and using mass selective detection of the ions. In this experiment we use a third laser tuned to the Balmer- α transition at 656 nm to induce one-photon-resonant two-photon ionization of the $n=2$ atoms. An advantage of this technique is that it will not ionize molecules in the E state, which would cause a background in the molecular ion signal.

The bandwidth of the radiation which drives the two-photon transition in this experiment is much narrower than the Doppler width of the transition. This results in excitation of only those molecules which have a narrow range of components of velocity along the beam. The second laser beam irradiates the molecules several nanoseconds later; if there have been no velocity-changing collisions in this time, as the second laser is scanned a Doppler-free excitation spectrum will be observed. The velocity-changing collision rate for H_2 in the E state is on the order of 10^5 s^{-1} under our experimental conditions, so velocity-changing collisions are very unlikely within a few nanoseconds. The resonance widths in this case will be determined by the ratio of the 201.7-nm laser bandwidth and the Doppler width of the two-photon transition. The resonance positions will be shifted by an amount $\Delta\nu = \delta(\nu_2/\nu_1)$ where δ is the detuning of the first laser from the center of the two-photon resonance, and ν_1 and ν_2 are the frequencies of the first and second lasers,

respectively.

The laser system used to generate the wavelengths required for the experiment is shown schematically in Fig. 2. The second harmonic of the output of a pulsed Nd-YAG laser (Quanta-Ray DCR-2; YAG is yttrium aluminum garnet) pumps a modified Littman dye-laser oscillator¹⁸ operating at 606.6 nm, with an output bandwidth ($\Delta E/hc$) of about 0.02 cm^{-1} and a duration of several nanoseconds. The dye-laser output goes through three longitudinally pumped amplifiers, reaching an energy of about 30 mJ. The output is frequency doubled in a 30-mm-long angle-tuned potassium dihydrogen phosphate (KDP) crystal and focused into a hydrogen Raman shifter with a 500-mm-focal-length lens. The various anti-Stokes components of the output are recollimated with a quartz lens and dispersed by a constant-deviation prism. The fourth anti-Stokes beam at 201.7 nm, with $\sim 10 \mu\text{J}$ pulse energy and a bandwidth of $\sim 0.15 \text{ cm}^{-1}$, is selected and focused into the experimental chamber with a 500-mm-focal-length lens.¹⁹

The third harmonic of the Nd-YAG laser pumps a second modified Littman oscillator²⁰ operating at wavelengths around 398.0 nm with a bandwidth of about 0.06 cm^{-1} . The output of this oscillator is amplified, resulting in pulse energies of about 1 mJ. This dye-laser beam is sent into the chamber unfocused and overlaps the first

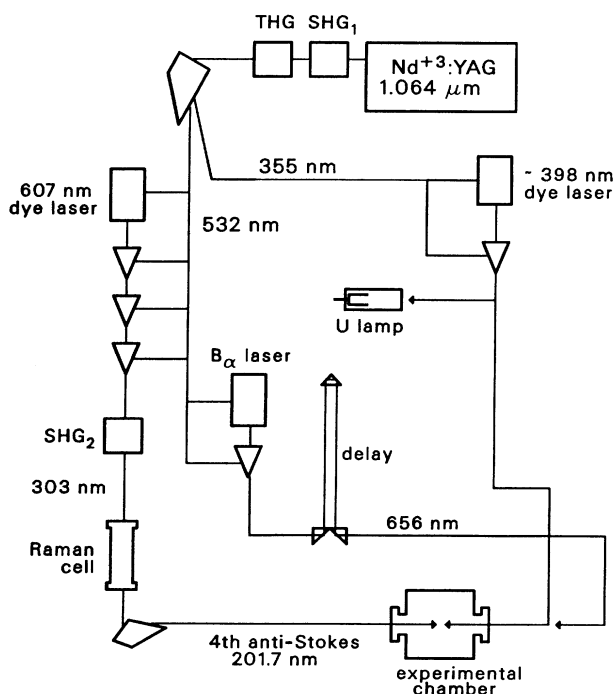


FIG. 2. Diagram of the laser system used to produce the wavelengths needed for two-step, two-color excitation of hydrogen Rydberg states and detection of dissociation products. SHG_1 is a KDP doubling crystal to produce 532 nm light, THG is a KDP mixing crystal to produce 355 nm light, and SHG_2 is a KDP doubling crystal to produce 303 nm light. The Raman cell is filled with H_2 to a pressure of 0.5 MPa.

beam in a counterpropagating, collinear arrangement. A fraction of the second harmonic of the Nd-YAG output is used to pump a third dye-laser oscillator (NRG type DL-0.03/20) operating at 656.3 nm with a bandwidth of 3 cm^{-1} , whose output is amplified to a pulse energy of $500 \mu\text{J}$ and focused into the interaction region in the experimental chamber with a 1000 mm focal length lens.

The photon energy in the beam which excites the Rydberg states is calibrated by splitting off a small fraction of the beam and directing it into a uranium hollow-cathode lamp. An optogalvanic spectrum of uranium transitions²¹ is thus acquired simultaneously with the ionization spectrum of the molecular hydrogen. For a typical run about seven uranium line positions are used in a nonlinear least-squares fit to a linear plus quadratic function of wavelength versus stepper-motor position. The energies of the uranium lines are taken from an atlas created at Los Alamos National Laboratory.²² The standard deviation of the actual energies from the fitted values is less than 0.03 cm^{-1} . This allows us to calibrate the photon energy to within 0.03 cm^{-1} . The wavelength of the 201.7 nm radiation is measured using the 9.15-m Paschen-Runge spectrometer in our laboratory.²³ The laser wavelength in third order of the spectrograph grating is compared to thorium standards in second order; in this scheme, the accuracy of the measurement is limited by variations in the conditions of the air in the spectrograph. For the conditions of air temperature, pressure, and humidity in our laboratory the accuracy of this measurement is about 0.05 cm^{-1} . This measurement allows us to correct the observed Doppler-free resonance positions to an accuracy of $\pm 0.02 \text{ cm}^{-1}$. The overall accuracy of our photon-energy measurements is thus about 0.05 cm^{-1} .

The energies of the levels of the E state which are needed to determine the absolute energies of the Rydberg states have been measured in our laboratory with an accuracy of 0.04 cm^{-1} . These measurements will be the subject of a separate communication.²⁴ The overall uncertainty in the absolute energies of the Rydberg states is $\sim 0.08 \text{ cm}^{-1}$.

The chamber which contains the hydrogen sample is designed to allow us to perform the experiment at relatively high pressures $\sim 13 \text{ Pa}$ (100 mTorr) and retain the ability to perform ion mass analysis. Ultrahigh-purity hydrogen flows through a palladium leak into a ballast, and out of the ballast into the sample chamber through a long, thin glass capillary. The chamber is equipped with two parallel plates, one of which has a 0.5-mm hole that opens into a 1-m-long differentially pumped drift tube. The pressure in the drift tube is maintained below 2 mPa (15 μTorr) with a 110-liter/s turbomolecular pump. The other plate is connected to a pulsed high-voltage power supply that is triggered by the laser, and provides a pulse of variable voltage, duration, and delay. For the study described here, the pulse is delayed by about 100 ns from the laser pulse to be certain that there is no electric field in the chamber when the laser excitation of the easily perturbed Rydberg states occurs. The electric field in the interaction region is estimated to be less than 2 V/m (0.02 V/cm) when the laser pulses arrive. Ions produced by the lasers are driven by the electric field through the small

hole in one plate into the field-free drift tube, which serves as a time-of-flight mass spectrometer. The ions are detected by a Galileo model No. TOF-2003 microchannel plate detector. The current from the detector is integrated by an Ortec model No. 142 charge-sensitive preamplifier whose output is amplified by an Ortec model No. 572 spectroscopy amplifier. The amplified signal is fed into two channels of a EG&G model No. 4420 boxcar averager controlled by a EG&G model No. 4402 signal processor. The timing of the gates on the two channels is adjusted so that one channel reads the H^+ signal while the other reads the H_2^+ signal. The amplified optogalvanic signal from the uranium lamp is sent into a third channel of the boxcar averager. The operating pressure in the chamber is between 130 mPa and 13 Pa (1 and 100 mTorr).

An LSI 11/73 microcomputer controls the experiment. In the course of a run, the laser which excites the Rydberg states is tuned using a stepping motor. Between steps the computer acquires data for 20 laser shots, averages the results for each channel, and then writes the results to a disk for storage. The stepping-motor step size is chosen so that the corresponding change in the laser wavelength is less than the linewidth of the 398 nm dye laser. The computer moves the motor a predetermined number of times to cover the spectral range of interest, thus generating a spectrum of the Rydberg states. In this study we were not concerned with absolute line strengths and the laser intensities were fairly stable; therefore, no normalization for variations in the intensities of the lasers has been performed.

II. RESULTS AND DISCUSSION

A. High singlet Rydberg state energies and analysis

We have used the techniques and equipment described above to observe excitation spectra of the singlet np Rydberg series which converge to the $v=0$, $N=0, 1, 2, 3$ states of the molecular ion, where N is the rotational quantum number of the ionic core. We have also observed Beutler-Fano profiles of $v=1$ autoionizing resonances with high resolution, but we will defer discussion of these results to a separate communication. The $N=0$ series of parahydrogen and the $N=1$ series of orthohydrogen are energetically forbidden to autoionize for all principle quantum numbers, and thus show sharp resonances over their entire Rydberg series. Therefore we are able to observe these series up to very high principle quantum number, and make accurate determinations of the series limits.

The accuracy to which ionization limits can be determined from analysis of the energies of Rydberg states increases as higher principle quantum number states are included, for several reasons. First, high Rydberg states lie very close to each other in energy; therefore, a large number of states can be measured in a small region of energy. These states also lie very close to the ionization limit, so that the distance in energy that one must extrapolate to reach the series limit is small. Perhaps most importantly, the effects of perturbations due to states of other Rydberg series is minimized by using states of high principle quantum number. There are two reasons for this. Since the interaction matrix elements which couple the Rydberg

states to low lying states of other series depend on the normalization factor of the Rydberg state, they become small as $n^{-3/2}$ for highly excited states. Also, the fact that the high Rydberg states lie in a small region of energy reduces the number of perturbing states that must be taken into account.

B. Parahydrogen ($J=1$ Rydberg series)

Figure 3 shows a scan of the $R(0)$ Rydberg series excited from the $v=0, J=0$ level of the E -state, taken at a pressure of 1.7 Pa (13 mTorr). The excited Rydberg molecules have been ionized by pulsed field ionization using a field of about 45 kV/m (450 V/cm). The scan shows resonances up to $n \sim 90$ where the Rydberg states are no longer resolved. The resonances typically have widths of $\sim 0.15 \text{ cm}^{-1}$, due to the laser linewidth (0.06 cm^{-1}), residual Doppler broadening ($\sim 0.06 \text{ cm}^{-1}$), and possible collisional broadening. We have seen no evidence of resonances due to transitions to states of higher angular momentum; this is to be expected since the inner well of the E, F potential has almost purely $2s\sigma$ character. We have measured the absolute energies of each of the Rydberg states observed in this scan to an accuracy of 0.08 cm^{-1} . The measured energies above the $v=0, J=0$ level of the ground state and effective quantum numbers of the observed parahydrogen Rydberg states are presented in Table I.

Analysis of this series to determine the ionization potential of the molecule is complicated by the presence of the series converging to the $N=2$ rotational level of the ionic core. The $N=2$ series of parahydrogen is known to be much weaker in excitation than the $N=0$ series, manifesting itself through its strong $\Delta v=0$ perturbation of the energies and intensities of the $N=0$ transitions and as a series of window resonances in the $N=0$ continuum. Multichannel quantum defect (MQDT) theory may be used to account for the perturbations in a simple and elegant way,^{1,25} and we have used this theory to analyze the $R(0)$ series.

MQDT predicts the energies of the states of both of the interacting Rydberg series in terms of their effective principle quantum numbers n_0^* and n_2^* , respectively. The predicted energies may be found by solving the simultaneous equations

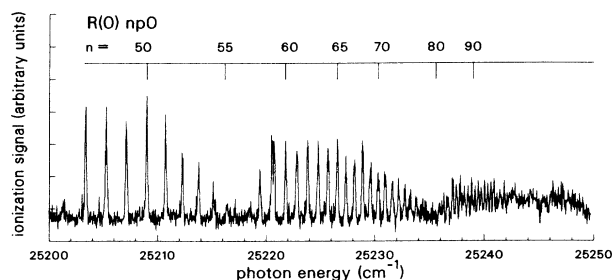


FIG. 3. $R(0)$ Rydberg series excited from the $v=0, J=0$ level of the E state (parahydrogen).

$$6B_0 = (\mathcal{R})_{H_2} \left[\frac{1}{(n_2^*)^2} - \frac{1}{(n_0^*)^2} \right], \quad (1)$$

$$\begin{vmatrix} -\sqrt{\frac{2}{3}} \sin[\pi(\delta_\sigma + n_2^*)] & \sqrt{\frac{1}{3}} \sin[\pi(\delta_\pi + n_2^*)] \\ \sqrt{\frac{1}{3}} \sin[\pi(\delta_\sigma - \delta_0^*)] & \sqrt{\frac{2}{3}} \sin[\pi(\delta_\pi - \delta_0^*)] \end{vmatrix} = 0, \quad (2)$$

where $6B_0$ is the energy difference between the $N=0$ and $N=2$ series limits, \mathcal{R} is the Rydberg constant, δ_π is the quantum defect for the Hund's case- b $np\pi$ states, δ_σ is the quantum defect for the $np\sigma$ states, and $\delta_0^* = n - n_0^*$. The quantum defect δ_π is determined from the $Q(1)$ series of orthohydrogen as described in Sec. II C of this paper. The procedure used in our analysis consists of a three-parameter fit of the MQDT predictions to our data: the parameters are δ_σ , B_0 , and the $N=0$ ionization potential. We estimate the uncertainty in the determination of the

TABLE I. Observed energies of Rydberg-state transitions in parahydrogen.

Excitation energy (cm ⁻¹) ^a	State assignment	
	$R(0)$	n_0^*
124 366.05	46	46.1257
124 368.09	47	47.0666
124 369.98	48	47.9932
124 371.85	49	48.9619
124 373.70	50	49.9866
124 375.43	51	50.9948
124 376.96	52	51.9493
124 378.46	53	52.9324
124 379.84	54	53.8870
124 381.08	55	54.7952
124 383.19	56	56.4535
124 384.05	57	57.1730
124 385.15	58	58.1282
124 386.18	59	59.0756
124 387.20	60	60.0580
124 388.17	61	61.0413
124 389.11	62	62.0418
124 390.01	63	63.0372
124 390.87	64	64.0473
124 391.63	65	64.9697
124 392.39	66	65.9488
124 393.13	67	66.9353
124 393.85	68	67.9516
124 394.56	69	68.9857
124 395.20	70	69.9700
124 395.84	71	70.9879
124 396.45	72	71.9851
124 396.99	73	72.9370
124 397.52	74	73.8963
124 398.07	75	74.9291
124 398.74	76	76.2477
124 400.96	81	81.1669
124 401.43	82	82.3422
124 401.78	83	83.2344

^aThe energy of the $E(v=0, J=0)$ level is taken to be 99 164.88 cm⁻¹.

photon energy at the series limit to be ± 0.03 cm⁻¹. The results, taking the $E(v=0, J=0)$ energy to be 99 164.88 \pm 0.04 cm⁻¹, are

$$\delta_\pi = -0.082,$$

$$\delta_\sigma = 0.196,$$

$$B_0 = 29.1 \text{ cm}^{-1},$$

and

$$(V_{IP})_{N=0} = 124 417.61 \pm 0.07 \text{ cm}^{-1}.$$

The result for the $N=0$ ionization potential V_{IP} agrees with a very recent result reported by another group,⁸ with an uncertainty which is smaller by a factor of three. The most recent theoretical result is also in good agreement with this number.²⁶ The other results all agree well with those of previous studies. It should be noted that much of the uncertainty in the result for the ionization potential resides in the value for the energy of the initial E -state level; thus, an improved determination of this energy would immediately allow us to derive a more accurate value for the ionization potential.

Figure 4 shows the energy differences between the theoretical and experimental values, with the position of the state responsible for the only $\Delta v \neq 0$ perturbation in this energy range indicated. It can be seen from this figure that the effects of this additional perturber are very small for Rydberg states of high principle quantum number, and should not affect the accuracy of our results in any significant way.

C. Orthohydrogen

The excitation spectrum of orthohydrogen prepared in the $E(v=0, J=1)$ level observed by electric field ionization using a field strength of 45 kV/m is shown in Fig. 5. For relatively low principle quantum number the $Q(1)$, $R(1)$, and $P(1)$ series are well resolved. The series which extends to the highest principle quantum numbers is the

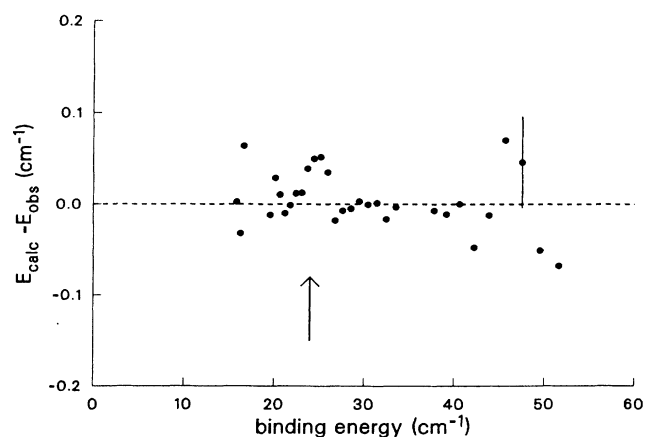


FIG. 4. The differences between the experimental energies and the energies predicted by MQDT. For simplicity, only one error bar is shown. The arrow denotes the position of the perturbing state $R(0) 3p\pi, v=6$.

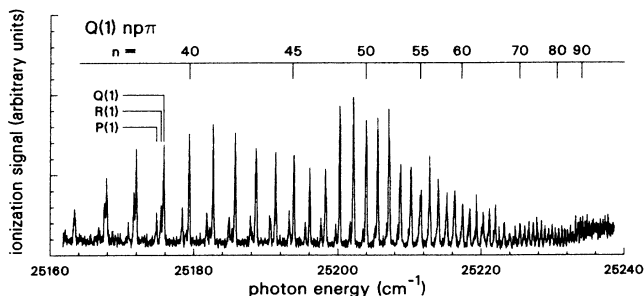


FIG. 5. Rydberg series excited from the $v=0, J=1$ level of the E state (ortho-hydrogen).

$Q(1) np\pi$ series, with resolved resonances extending to $n \sim 90$. Since there is only one $J=1$ ortho level possible for a given vibrational quantum number, the $Q(1)$ series is free of $\Delta v=0$ perturbations. For this reason, we have used the $Q(1)$ series in the determination of the $N=1$ series limit and the quantum defect δ_π . Table II gives our results for the energies of the observed high Rydberg transitions, relative to the $J=1$ level of the ground state.

Since the effects of any $\Delta v \neq 0$ perturbations are small, we analyzed the spectrum by fitting the experimental points to a Balmer formula with the parameters being the $N=1$ ionization potential and the quantum defect δ_π . Figure 6 shows the differences between the observed energies of the $Q(1)$ series and energies calculated using $\delta_\pi = -0.082$ and a value of the $N=1$ series limit photon energy of $25\,247.68 \text{ cm}^{-1}$. The positions of states responsible for $\Delta v \neq 0$ perturbations are indicated, and their effects are seen to be small. The fact that our observations extend up to very high principle quantum numbers minimizes the effects of perturbations and results in a very accurate determination of the photon energy corresponding to the series limit, accurate to within $\pm 0.03 \text{ cm}^{-1}$. The addition of the rotational energy of the ground state²⁷ (118.49 cm^{-1}) and our measured value of the two-photon

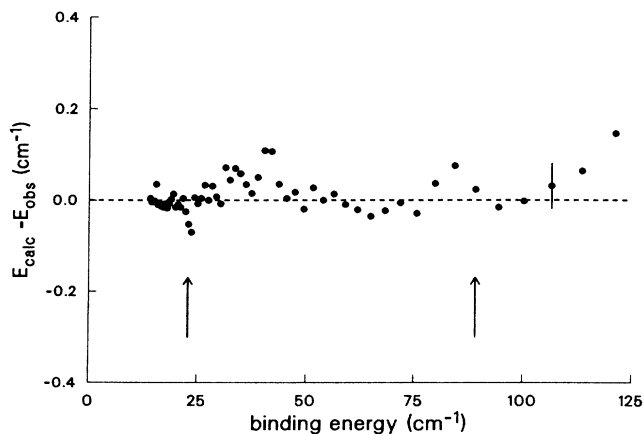


FIG. 6. The differences between the observed energies of the $Q(1)$ ortho-hydrogen series and energies calculated from a Balmer formula using a quantum defect of -0.082 and the experimentally determined ortho-hydrogen series limit. The arrows denote the positions of two perturbations: $R(1) 4p\sigma, v=4$ at 22.9 cm^{-1} , and $R(1) 7p\sigma, v=1$ at 89.1 cm^{-1} .

transition energy ($99\,109.77 \pm 0.04 \text{ cm}^{-1}$) to the photon energy results in a value for the $N=1$ ionization potential referred to the $v=0, J=0$ level of the ground state of $124\,475.94 \pm 0.07 \text{ cm}^{-1}$. This result agrees with previous results,¹ and is more accurate by a factor of three.

D. Predissociation of high Rydberg states

There have been a number of studies of predissociation of low-lying states of molecular hydrogen, generally involving the derivation of predissociation yields from observed line shapes or detection of fluorescence from dissociation products.^{5,28–30} Predissociation of high Rydberg states has not been observed until this study.

We have observed significant predissociation rates for ortho-hydrogen Rydberg states with principle quantum numbers up to $n \sim 50$. Figure 7 shows a comparison of simultaneously acquired H^+ and H_2^+ spectra taken at a pressure of 12 Pa (90 mTorr) with a pulsed field strength of 18 kV/m . At this relatively high pressure there is a considerable degree of collisional ionization of the Rydberg-state populations; indeed, this process is responsible for the molecular ion signal for $n < 37$. Above $n=36$ the pulsed field ionizes all of the population remaining after 100 ns . The laser tuned to the Balmer- α transition ionizes about 20% of the $\text{H}(2s)$ atoms produced by predissociation. The spectra have not been corrected for variations in laser intensity over the scan range or for possible differences in detection efficiency for the two ionic species; therefore, no absolute branching ratios for the various decay processes can be derived from the present data. However, we can draw some qualitative conclusions from the data.

The Rydberg states in this range of principle quantum number show a wide range of predissociation rates. This is clearly illustrated in the $n=25$ transitions, which can either be collisionally ionized or predissociate. The $P(1) 25p\sigma$ transition is observed strongly in predissociation and hardly at all in ionization, whereas the $R(1) 25p1$ transition is seen strongly in ionization and very weakly in predissociation. This complementarity is a general feature of the spectra. One explanation for this situation is that

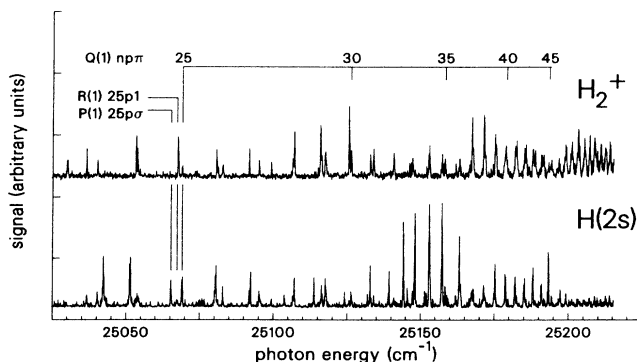


FIG. 7. Simultaneously acquired spectra of ionization and predissociation for the high Rydberg states of ortho-hydrogen. The spectra are offset for clarity.

TABLE II. Observed energies of Rydberg-state transitions in orthohydrogen.

Excitation energy (cm ⁻¹) ^a	Q(1)	State assignment		n [*]
		R(1)	P(1)	
124 236.07	30			30.0637
124 243.83	31			31.0731
124 250.83	32			32.0772
124 257.21	33			33.0825
124 263.02	34			34.0847
124 268.29	35			35.0775
124 273.11	36			36.0659
124 276.53			37	36.8210
124 277.37		37		37.0127
124 277.63	37			37.0733
124 280.68			38	37.8032
124 281.47		38		37.9976
124 281.83	38			38.0892
124 284.62			39	38.8112
124 285.26		39		38.9820
124 285.63	39			39.0836
124 288.26			40	39.8186
124 288.78		40		39.9695
124 289.19	40			40.0888
124 291.64			41	40.8292
124 292.06		41		40.9607
124 292.48	41			41.0934
124 294.66			42	41.7974
124 295.05		42		41.9312
124 295.52	42			42.0890
124 297.59			43	42.8100
124 298.35	43			43.0856
124 300.30			44	43.8115
124 300.98	44			44.0764
124 302.80			45	44.8077
124 303.47	45			45.0817
124 305.13			46	45.7889
124 305.76	46			46.0699
124 307.38			47	46.8071
124 307.98	47			47.0917
124 309.43			48	47.7988
124 309.98	48			48.0735
124 311.35			49	48.7830
124 311.91	49			49.0804
124 313.26			50	49.8256
124 313.67	50			50.0615
124 314.91			51	50.7872
124 315.30	51			51.0173
124 316.90	52			52.0113
124 318.46	53			53.0472
124 319.93	54			54.0713
124 321.26	55			55.0559
124 322.51	56			56.0351
124 323.71	57			57.0222
124 324.88	58			58.0426
124 325.95	59			59.0134
124 327.07	60			60.0904
124 328.04	61			61.0739
124 328.95	62			62.0480
124 329.88	63			63.0810
124 330.70	64			64.0434
124 331.55	65			65.0778
124 332.34	66			66.0921
124 333.06	67			67.0748
124 333.85	68			68.1843

TABLE II. (Continued).

Excitation energy (cm^{-1}) ^a	$Q(1)$	State assignment		n_i^*
		$R(1)$	$P(1)$	
124 334.52	69			69.1614
124 335.14	70			70.1205
124 335.73	71			71.0765
124 336.35	72			72.1078
124 336.92	73			73.0989
124 337.48	74			74.1106
124 337.98	75			75.0559
124 338.49	76			76.0775
124 338.99	77			77.0970
124 339.48	78			78.1206
124 339.91	79			79.0977
124 340.36	80			80.1172
124 340.77	81			81.1150
124 341.17	82			82.1020
124 341.56	83			83.1053
124 341.90	84			83.9876
124 342.30	85			85.0848
124 342.65	86			86.0946
124 342.98	87			87.0948
124 343.30	88			88.0693

^aThe energy of the $X(v=0, J=1) \rightarrow E(v=0, J=1)$ transition is taken to be $99\,109.77 \text{ cm}^{-1}$.

the two processes compete for the Rydberg state population: if one process or the other occurs with a much greater rate, the Rydberg state will be observed to decay mainly through that channel due to depletion of the excited state. It should also be noted that qualitatively the predissociation rate will reflect the degree of admixture of the state in question with states of lower principle quantum number; the greater the admixture, the higher the probability that the excited electron will scatter off the ionic core causing a transfer of the nuclear motion to an unbound potential curve, leading to dissociation. Conversely, the collisional ionization rate would be expected to reflect the high principle quantum number content of the state, since it is from this component that collisions can ionize the molecule with high probability. Thus the complementarity of the two processes may be due to variations in the compositions of the Rydberg states for different branches as the principle quantum number increases.

In the energy region presented in Fig. 7 there are several regions in which the predissociation of some states becomes strong, in particular, near $n=24$ and 34 . This indicates to us the presence near these energies of strongly predissociated perturbing states of low principle quantum number, which are not directly excited but mix with the high Rydberg states leading to large predissociation rates for some of them. High vibrational levels of the B and D'' states have previously been observed near these energies,³ and are good candidates for the perturbers. This process of predissociation by coupling to a discrete predissociated state which by "accident" is nearly degenerate with the state of interest, rather than by direct coupling to a dissociative continuum, has been noted previously for low-lying $np\pi$ states.⁵

III. CONCLUSION

We have used two-step, two-color excitation with two-photon resonance to excite molecular hydrogen to singlet np Rydberg states of very high principle quantum number; using this scheme, we have measured the Rydberg-state energies with high accuracy. Analysis of the measured energies has yielded very accurate results for the lowest ionization potentials of the E state of para- and orthohydrogen; by combining these results with our measurements of the E -state level energies, we have derived the most precise values to date for the energies of the lowest two ionization limits of the ground state of the hydrogen molecule. The techniques used in this experiment can be extended to other molecular systems for which accurate ionization potentials are not available. Strong predissociation of some of the Rydberg states has been observed, apparently due to perturbations by predissociated states of low principle quantum number.

We are in the process of extending the Rydberg-state studies described here to the other isotopic forms of molecular hydrogen. We will also observe Rydberg-state predissociation at higher resolution, and determine rates and branching ratios into the various decay paths open to the Rydberg states. This information will allow us to unambiguously determine the source of the predissociation and provide accurate quantitative results with which to test a theoretical treatment of the problem.

ACKNOWLEDGMENTS

The expert technical help of Bert Ercoli and Al Svirnickas is gratefully acknowledged. This research was supported by the U.S. Department of Energy under Contract No. GC-01-01-06-1.

- ¹G. Herzberg and Ch. Jungen, *J. Mol. Spectrosc.* **41**, 425 (1972).
²S. Takezawa, *J. Chem. Phys.* **52**, 2575 (1970).
³W. A. Chupka and J. Berkowitz, *J. Chem. Phys.* **51**, 4244 (1969).
⁴P. M. Dehmer and W. A. Chupka, *J. Chem. Phys.* **65**, 2243 (1976).
⁵M. Glass-Maujean, J. Breton, and P. M. Guyon, *Chem. Phys. Lett.* **63**, 591 (1979).
⁶R. D. Knight and L. Wang, *Phys. Rev. Lett.* **55**, 1571 (1985).
⁷R. Kachru and H. Helm, *Phys. Rev. Lett.* **55**, 1575 (1985).
⁸E. E. Eyler, R. C. Short, and F. M. Pipkin, *Phys. Rev. Lett.* **56**, 2602 (1986).
⁹N. Bjerre, R. Kachru, and H. Helm, *Phys. Rev. A* **31**, 1206 (1985).
¹⁰H. Rottke and K. H. Welge, *J. Phys. (Paris)* **46**, C1-127 (1985).
¹¹S. T. Pratt, P. M. Dehmer, and J. L. Dehmer, *Chem. Phys. Lett.* **105**, 28 (1984).
¹²E. E. Marinaro, C. T. Rettner, R. N. Zare, and A. H. Kung, *Chem. Phys. Lett.* **95**, 486 (1983).
¹³C. Cornaggia, D. Normand, J. Morellec, G. Mainfray, and C. Manus, *Phys. Rev. A* **34**, 207 (1986).
¹⁴E. E. Marinaro, R. Vasudev, and R. N. Zare, *J. Chem. Phys.* **78**, 692 (1983).
¹⁵D. W. Chandler and L. R. Thorne, *J. Chem. Phys.* **85**, 1733 (1986).
¹⁶R. S. Freund, in *Rydberg States of Atoms and Molecules*, edited by R. F. Stebbings and F. B. Dunning (Cambridge University Press, Cambridge, England, 1983), p.383.
¹⁷R. S. Berry and S. E. Nielsen, *Phys. Rev. A* **1**, 383, 395 (1970).
¹⁸R. Mahon and F. S. Tompkins, *IEEE J. Quantum Electron.* **QE-18**, 913 (1982).
¹⁹W. L. Glab and J. P. Hessler (unpublished).
²⁰J. F. Kelly, J. P. Hessler, and G. Alber, *Phys. Rev. A* **33**, 3913 (1986).
²¹D. S. King, P. K. Schenck, K. C. Smyth, and J. C. Travis, *Appl. Opt.* **16**, 2617 (1977).
²²B. A. Palmer, R. Engleman, Jr., and E. F. Zalewski, An Atlas of Uranium Emission Intensities in a Hollow Cathode Discharge, Los Alamos Scientific Laboratory Report No. LA-8251-MS (unpublished).
²³F. S. Tompkins and M. Fred, *Appl. Opt.* **2**, 715 (1963).
²⁴J. P. Hessler and W. L. Glab (unpublished).
²⁵U. Fano, *Phys. Rev. A* **2**, 353 (1970).
²⁶ $V_{IP}(N=0)=124\,417.50\text{ cm}^{-1}$, obtained from the results of the following two papers: D. M. Bishop and L. M. Cheung, *J. Chem. Phys.* **69**, 1881 (1978) (ground state of H_2^+); and W. Kolos, K. Szalewicz, and H. J. Monkhorst, *J. Chem. Phys.* **84**, 3278 (1986) (dissociation energy of H_2).
²⁷K. Huber and G. Herzberg, *Constants of Diatomic Molecules* (Van Nostrand Reinhold, New York, 1979).
²⁸P. M. Guyon, J. Breton, and M. Glass-Maujean, *Chem. Phys. Lett.* **68**, 314 (1979).
²⁹M. Rothschild, H. Egger, R. T. Hawkins, H. Pummer, and C. K. Rhodes, *Chem. Phys. Lett.* **72**, 404 (1980).
³⁰J. H. M. Bonnie, P. J. Eenshuistra, J. Los, and H. J. Hopman, *Chem. Phys. Lett.* **125**, 27 (1986).